J Digit Imaging (2013) 26:748–758
DOI 10.1007/s10278-012-9555-6

A Modified Undecimated Discrete Wavelet Transform Based Approach to Mammographic Image Denoising

Eri Matsuyama · Du-Yih Tsai · Yongbum Lee · Masaki Tsurumaki · Noriyuki Takahashi · Haruyuki Watanabe · Hsian-Min Chen

Published online: 1 December 2012

Abstract In this work, the authors present an effective denoising method to attempt reducing the noise in mammographic images. The method is based on using hierarchical correlation of the coefficients of discrete stationary wavelet transforms. The features of the proposed technique include iterative use of undecimated multi-directional wavelet transforms at adjacent scales. To validate the proposed method, computer simulations were conducted, followed by its applications to clinical mammograms. Mutual information originating from information theory was used as an evaluation measure for selection of an optimal wavelet basis function. We examined the performance of the proposed method by comparing it with the conventional undecimated discrete wavelet transform (UDWT) method in terms of processing time-consuming and image quality. Our results showed that with the use of the proposed method the computation time can be reduced to approximately 1/10 of the conventional UDWT method consumed. The results of visual assessment indicated that the images processed with the proposed UDWT method showed statistically significant superior image quality over those processed with the conventional UDWT method. Our research results demonstrate the superiority and effectiveness of the proposed approach.

E. Matsuyama · D.-Y. Tsai (✉) · Y. Lee · H. Watanabe
Department of Radiological Technology, Graduate School of Health Sciences, Niigata University, 2-746, Asahimachi-dori, Niigata 951-8518, Japan
e-mail: tsai@clg.niigata-u.ac.jp

M. Tsurumaki
Department of Radiology, Nakajo Central Hospital, Niigata, Japan

N. Takahashi
Department of Radiology, Sendai City Hospital, Sendai, Japan

H.-M. Chen
Department of Biomedical Engineering, Hungkuang University, Taichung, Taiwan

Keywords Medical imaging · Mammograms · Wavelet transform · Image quality · Denoising

Introduction

Breast cancer is one of the leading causes for cancer mortality among women and continues to be a significant public health problem in the world [1, 2]. Mammography is one of the most effective and reliable methods for early breast cancer detection [3–6]. However, mammography is still far from being ideal, with its sensitivity only ranging from 70 % to 90 % [7]. The clinical significance of early breast cancer diagnosis and a clear need to reduce false–negative rate of screening mammography have motivated the development of computer-aided detection (CADe) systems for decision support [8–17]. These systems typically involve a series of steps; first applying a variety of image preprocessing to reduce the noise and/or to enhance suspicious structures in the image and then using morphological and textural analysis to better differentiate these structure between true positives and false positives. Thus image preprocessing plays a key role in extracting the characteristic features of images to implement CADe system classification. The main image processing techniques applied for mammography could be used to smooth noise, equalize systematic variations in density or gray level, and enhance local contrast and sharpness of calcifications. Image processing has indeed been suggested as a way to improve performance of digital mammography [18, 19].

Noise removal is one of the most common and important processing steps in CADe systems for mammography. Because of its importance, there has been an enormous amount of research dedicated to the subject of noise removal and many methods have been proposed [20–33]. Several approaches have been proposed with the use of discrete

wavelet transform (DWT) [30, 31, 34, 35]. The DWT is very efficient from the computational point of view, but it is shift variant. Thus its denoising performance can change drastically if the starting position of the signal is shifted. In order to achieve the shift invariance and to get more complete characteristic of the analyzed signal, the undecimated DWT (UDWT) has been proposed [36–39]. Mencattini et al. developed methods for the reduction of noise in mammographic images, based on UDWT using subband noise variance computation both for homoscedastic and heteroscedastic noise [40, 41]. The reported methods were robust and effective. But, the methods were not advantageous from computational aspects. Zhao et al. proposed an image denoising based on Gaussian and non-Gaussian distribution assumption for wavelet coefficients [42]. Huang et al. reported a denoising method by selecting the thresholds for denoising directly by evaluating some statistical properties of the noise [43]. Unfortunately, the assumption of a signal-independent, Gaussian, and homoscedastic noise may appear not suitable for medical images.

In the present study, we presented a modified UDWT approach to mammographic denoising both for improving image quality and for decreasing image processing time-consuming. The main features of the proposed method include the incorporation of the use of hierarchical correlation of the coefficients of the UDWT and iterative use of undecimated multi-directional wavelet transforms at two consecutive levels.

In this paper, we firstly conducted computer simulations for selection of an optimal wavelet basis function to perform wavelet analysis. In this simulation study, mutual information originating from information theory was used as an evaluation metric for the selection. After determination of an optimal wavelet basis function, we applied the proposed approach to 30 clinical mammograms for image denoising. We compared our results with those obtained from the conventional UDWT method. The validity of the proposed approach was verified by perceptual evaluation.

Materials and Methods

Undecimated Discrete Wavelet Transform Method

The UDWT has been discovered for various purposes and under different names, e.g., the shift/translation invariant wavelet transform, the stationary wavelet transform, or the redundant wavelet transform [39, 44]. The key point is that it is redundant, shift invariant, linear, and it gives a better approximation to the continuous wavelet transform than the approximation provided by the orthonormal discrete wavelet transform. Unlike the DWT, the UDWT does not incorporate the down sampling operations. Thus, the approximation coefficients (low-frequency coefficients) and detailed coefficients (high-frequency coefficients) at each level are the same length as the original signal.

The basic algorithm of the conventional UDWT is that it applies the transform at each point of the image and saves the detailed coefficients and uses the approximation coefficients for the next level. The size of the coefficients array does not diminish from level to level [36]. This decomposition is further iterated up to level 4. After computing the UDWT of the image, thresholding of the detailed coefficients at all levels using VisuShrink technique [45] is performed by applying the universal threshold proposed by Donoho and Johnstone [46]. The wavelet coefficients are subjected to soft thresholding, with threshold given by $t = \sigma \times \sqrt{2\log(n)}$, where σ is the standard deviation of the noise at level 1 and n is the size of the coefficient arrays [47]. The wavelet basis function used here was Daubechies order 2 (db2). The inverse UDWT is then computed to obtain the denoised image.

Proposed Method

Figure 1 shows the flowchart of our proposed method. The main steps are outlined below:

1) Apply the UDWT to the original image to produce wavelet coefficients up to level 2.
2) Compute the hierarchical correlations of the detailed coefficients (subbands) between level 1 and level 2 for the three different (horizontal, vertical, and diagonal) subbands, respectively. The hierarchical correlations for the three detailed subbands are given by:

$$\left| Coef_{lev\_1}(p,q)_{(H),(V),(D)} \times Coef_{lev\_2}(p,q)_{(H),(V),(D)} \right| \tag{1}$$

where p and q are the new coordinates after wavelet transform. $Coef_{lev\_1}$ and $Coef_{lev\_2}$ are wavelet coefficients of level 1 and 2. H, V, and D denote horizontal, vertical, and diagonal subbands, respectively.

3) Determine threshold values for each detailed subband based on the obtained hierarchical correlation values. The determination procedure is as follows:

   (a) Generate a correlation image $Img_{Cor}(p,q)$ for each detailed subband:

$$Im\,g_{Cor}(p,q)_{(H),(V),(D)} = |Coef_{lev\_1}(p,q)_{(H),(V),(D)} \times Coef_{lev\_2}(p,q)_{(H),(V),(D)}| \tag{2}$$

   (b) Find the maximum value in each row in the horizontal (x) direction of the obtained correlation image for

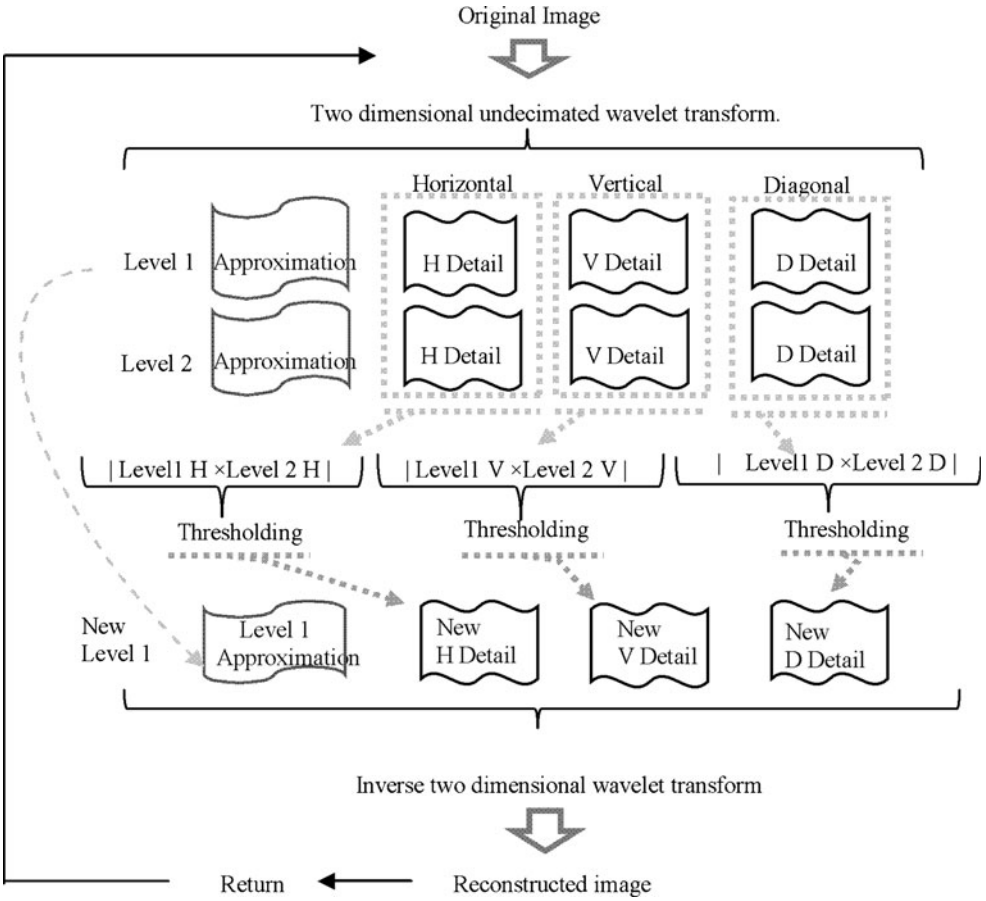

Fig. 1 Flow chart of the proposed method

each of the three detailed subbands, that is, high-frequency horizontal, vertical, and diagonal subbands.

(c) Calculate the mean of the maximum values obtained from all rows in the x direction of the correlation image. The mean is denoted by $\text{Mean}_{\max}$.

(d) Exclude those correlation values greater than $0.8 \times \text{Mean}_{\max}$. These excluded values are considered signal data. The value of 0.8 was determined empirically through experimentation.

(e) Calculate the standard deviation σ from the remaining correlation values.

(f) Determine the threshold value by using the formula:

$$THR = 1.6 \times \sigma \tag{3}$$

The value of 1.6 was determined empirically through experimentation.

4) Apply the determined threshold values to the correlation values:

$$New\ Coef_{lev\_1}(p,q) = \left\{ \begin{array}{ll} Coef_{lev\_1}(p,q), & if \quad |Coef_{lev\_1}(p,q) \times Coef_{lev\_2}(p,q)| \geq THR \\ 0, & otherwise \end{array} \right\}, \tag{4}$$

where $New\ Coef_{lev\_1}(p,q)$ is the newly obtained, modified coefficient for level 1. The modified coefficients of the horizontal, vertical, and diagonal subbands are respectively obtained. It should be noted that the threshold operation was only applied to the detailed components. The approximation component remains unchanged.

5) Apply inverse wavelet transform to reconstruct denoised image based on the approximation coefficients of level 1 and the three modified, detailed coefficients of level 1.

6) Repeat steps 1–5 one time to further remove the noise and lead to obtain a final denoised image.

The major differences between the proposed UDWT method and the conventional UDWT method are as follows. First, the conventional UDWT decomposed the original image (level 0) into one low-frequency band (low-low band; approximation coefficients) and three high-frequency bands (low–high, high–low, and high–high bands; detailed coefficients) for each resolution level with the same size as the original image. The decompositions are usually conducted up to resolution level 4. In contrast, the proposed UDWT method only needs to perform the computation up to resolution level 2 and repeat the computation one time. Second, the conventional UDWT thresholded the detailed coefficients at all 4 levels with the same thresholding value, while the proposed method utilized the hierarchical correlation of the coefficients between the level 1 and level 2 of the three detailed coefficients for thresholdings. That is, the thresholding values were various and dependent on the nature of the noise.

Computer Simulated Images

Computer simulated images were designed and used for selection of wavelet basis functions. The design framework is as follows. A simulated image $g(x,y)$ was given by a spatial convolution between a uniform-distributed signal (an object) $f(x,y)$ having intrinsic noise $u(x,y)$ and a blurring function B. If the external noise $v(x,y)$ was also taken into consideration, the resulting image could be represented by the following formula:

$$g(x,y) = \sum_{s=1}^{8} \{[s \times f(x,y) + u(x,y) \times W] * B + v(x,y) \times K\}, \tag{5}$$

where the symbol * represents the convolution operation and s is an integer representing the number of strips of the simulated image. The terms of W and K are weighting coefficients used to adjust noise level [48, 49].

In the simulation studies, the input image $f(x,y)$ consisted of 8 stripes with different width. The $u(x,y)$ and the $v(x,y)$ were Poission noise and Gaussian noise, respectively. We used an "$m \times m$" (m is an odd integer) averaging filter as the blurring function. The extent of blurring was adjusted by varying the filter size. Figure 2 shows two simulated images with different resolution, contrast and noise levels. The simulated images were regarded as different thickness of fibers, which realistically depicts one of the major signs of breast cancer in a mammogram.

Selection of Wavelet Basis Functions

We evaluated six different wavelet basis functions, namely, discrete FIR approximation of Meyer wavelet (dmey), Daubechies order 2 (db2), Symlets order 7 (sym7), Coiflets order 1 (coif1), Coiflets order 5 (coif5), and biorthogonal 6.8 (bior6.8), as candidates for selection as the most suitable basis function for the UDWT used in this study. The reason for pre-selecting the mentioned 6 basis functions was because they are comparatively popular wavelet basis functions used in the analysis of signals and images [50].

Mutual Information

In this work, we employed mutual information (MI) as a metric of image quality [48, 51] for selecting a suitable wavelet basis function to be incorporated in the proposed method. MI is used to express the amount of information that an output image contains about an input object. The more the MI value provides, the better the image quality is [48]. Therefore, the overall quality of an image can be quantitatively evaluated by measuring MI.

We briefly describe the theoretical framework utilized in this work for image quality assessment. A more detailed explanation of the theoretical constructs can be found in Refs. [48] and [51].

If a set of events a_1, a_2….. a_m whose probabilities are given by $\{p_1, p_2, \ldots\ldots p_m\}$, then the Shannon entropy H can be expressed as

$$H(P_1, P_2, \ldots P_m) = -\sum_{i=1}^{m} P_i \log_2 P_i. \tag{6}$$

Here, we consider that x and y as two random variables corresponding to an input variable and an output variable,

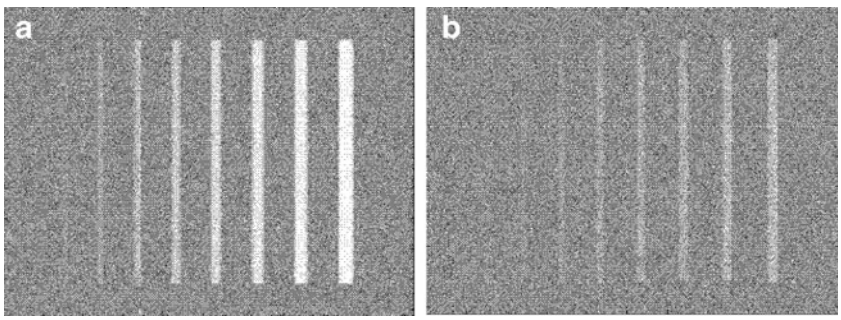

Fig. 2 Two computer-simulated images. **a** Image with higher contrast and lower noise level. **b** Image with lower contrast and higher noise level

Table 1 Comparison of three image quality measurements of 6 different wavelet basis functions for simulated noisy images

Image quality measurement	Wavelet basis function					
	dmey	db2	sym7	coif1	coif5	bior6.8
MI (bit)	0.68	0.81	0.72	0.79	0.69	0.72
MSE	58.43	50.20	55.87	51.01	57.1	55.51
SNR (dB)	27.93	29.10	28.21	28.93	28.04	28.29

MI: mutual information, *MSE*: mean square error, *SNR*: signal to noise ratio

respectively. In this case, the entropy for the input and that for the output can be denoted as $H(x)$ and $H(y)$, respectively. Then the mutual information, $MI(x;y)$, can be defined as follows:

$$MI(x;y) = H(x) - H_y(x) = H(y) - H_x(y) \\ = H(x) + H(y) - H(x,y), \quad (7)$$

where $H(x,y)$ is the joint entropy, and $H_x(y)$ and $H_y(x)$ are conditional entropies.

Consider an experiment in which every input has a unique output belonging to one of the various output categories. In this work, the inputs are considered to be a set of subjects—for example, a test sample object with steps of various thickness—whereas the outputs may be their corresponding images with various optical densities or gray levels. As shown in Eq. 7, MI carries the amount of information that output y has about input x.

If the output is identical to the input, then knowing the output provides complete information about the input. In this case, MI is maximized and equal to the input entropy, and the uncertainty of the input is reduced to 0. This means that knowing (or viewing) the image of an object (subject) receives complete information about the object (subject). Thus, the quality of the obtained image reaches to a maximum value in terms of MI. If, on the other hand, the output and the input are independent, then knowing the output does not help make any conclusions about the input. In this case, the MI value is zero, and therefore, the uncertainty about the input remains unchanged. This means that the obtained image has the lowest quality from the point of view of MI.

Image Dataset

Mammograms were obtained from the data base of the Japanese Society of Medical Imaging Technology [52]. The original screen-film mammograms were collected from several medical institutions and they were digitized using a film digitizer with a pixel size of 100×100 μm and 10-bit gray-level resolution. The size of each image was 2,510×2,000 pixels. A region of interest with a fixed size of 200×200 pixels was manually selected. A total of 30 mammograms (14 normal cases and 16 abnormal cases) obtained from the database were used for investigation of the effectiveness of the proposed method.

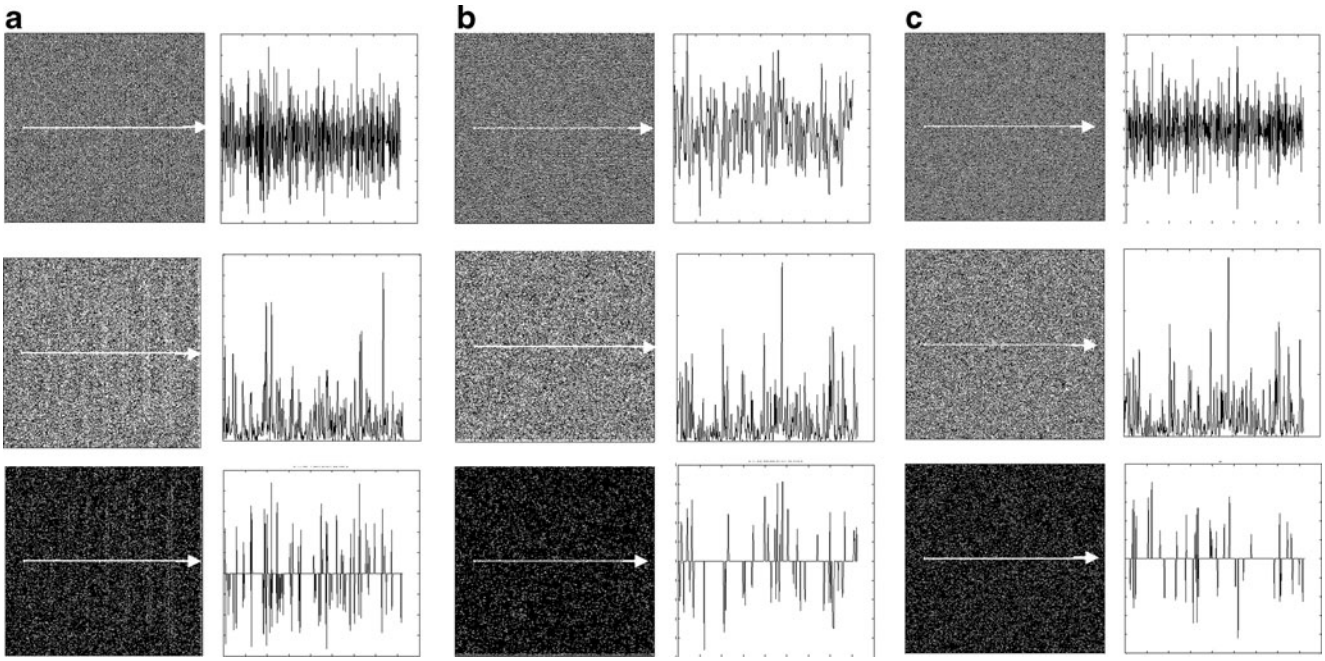

Fig. 3 An example showing images and plots of the three detailed coefficients. **a** Vertical, **b** horizontal, and **c** diagonal coefficients

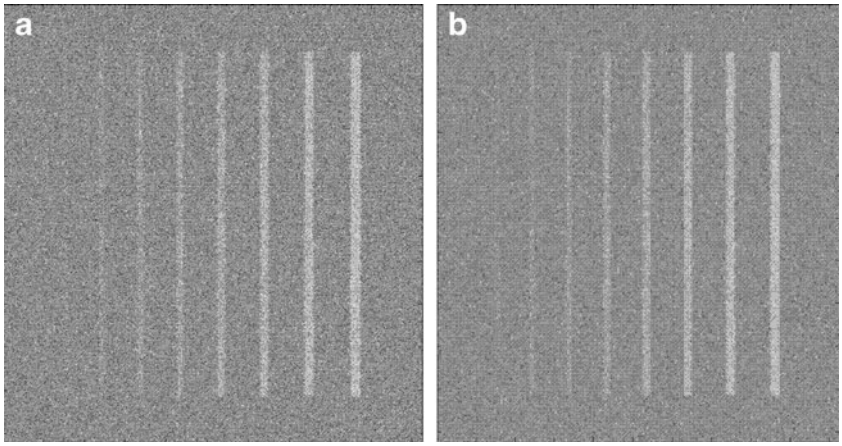

Fig. 4 Example of simulated noisy images before and after denoising. **a** Original simulated noisy image. **b** Image processed by the proposed UDWT method

Visual Evaluation

The obtained 30 mammograms were processed using both the proposed UDWT and the conventional UDWT methods. Thus, a total of 90 images including the original images were used for image quality valuation. In this study, Scheffe's method of paired comparison was employed for visual performance analysis [53, 54]. The visual evaluation was conducted by seven experienced radiological technologists (ranging from 15 to 25 years of experience). All images were evaluated on a pair of popular medical 3M monochrome liquid-crystal display (LCD) monitors (2,048×1,536 matrix, 700:1 contrast ratio, Mediotto, Nagano, Japan). To assure a consistent image on the monitors, all displays were calibrated to comply with the Digital Imaging and Communications in Medicine (DICOM) part 14: Grayscale Standard Display Function. Each observer reviewed the images independently. The reading time was limited to less than 20 s for each reading. The observers independently evaluated one pair of images, which were shown on the monitors at a time, using a 5-point grading scale (−2 points to +2 points). If the image shown on the left is much better than that shown on the right in terms of overall image quality, the left image is given +2 points; the left image is given +1 point when it is slightly better than the right one; the left image is given 0 point, when both images show the same image quality. In contrast, if the image shown on the left is much poorer than that shown on the right in terms of overall image quality, the left image is given −2 points; the left image is given −1 point when it is slightly poorer than the right one. Comparisons were made by use of three possible combinations, that is, original/conventional UDWT, original/proposed UDWT, and conventional UDWT/proposed UDWT combinations. Each pair of images was determined randomly. Also, the two separate images (left side vs. right side) were arranged on a random basis.

Results

Selection of Wavelet Basis Functions

The quality of the UDWT-processed simulated images was quantitatively assessed by use of the MI metric. We also employed two commonly used measurement parameters, mean square error (MSE), and signal to noise ratio (SNR) for comparison. In medical imaging, MSE is frequently used as a metric to evaluate the difference between a reference image and a noisy image or a processed image. The processed image with minimum MSE indicates that the image-processing method is the best. As it is seen, MSE needs two images for the calculation. In the present simulation studies, we used a noise-free simulated image as the reference image. As is well-known that a higher SNR value means that the signal strength is stronger in relation to the noise levels, thus the higher the SNR value the better the quality of the image is. Results for the simulated noisy images processed by the 6 wavelet basis functions are presented in Table 1. It is obvious from the table that the wavelet-processed image with db2 basis function gave the best result among the 6 basis functions in all three quality metrics. Thus, we selected db2 basis function for the proposed method.

Figure 3 shows an example of processing procedure of the proposed method for the simulated noisy images. Figure 3a–c

Table 2 Comparison of three image quality measurements for the simulated noisy images before and after image processing

MI: mutual information, *MSE*: mean square error, *SNR*: signal to noise ratio

Image quality measurement	Original simulated noisy image	Proposed UDWT-processed image	Conventional UDWT-processed image
MI (bit)	0.40	0.81	0.56
MSE	130.37	50.20	76.66
SNR (dB)	24.10	29.10	25.59

illustrates the in-progress status of the process for the vertical, horizontal and diagonal wavelet coefficients, respectively. For example, shown on the left column of the top row of Fig. 3a is the wavelet coefficients of subband at level 1 and on the right column is the x-direction profile of the coefficient distribution at the central pixels indicated on the image. Shown on the left column of the middle row is the correlation image depicting the correlation values between level 1 and level 2, and on the right column is the *x* direction profile of the correlation values at the central pixels indicated on the image. On the left column of the bottom row shows the image obtained from the newly modified coefficients of subbands at level 1 after performing the first iteration of the processing of the proposed method and shown on the right column corresponds to the *x* direction profile of the coefficient distribution at the central pixels. Similarly, Fig. 3b, c illustrates the in-progress status for the horizontal and diagonal coefficients, respectively. Looking at the initial coefficient distribution of level 1 (top row, left column) and the modified coefficient distribution (bottom row, right column) for each of the three detailed coefficients, it is obvious that the noise has been substantially removed.

Figure 4 shows an example of the simulated noisy images before and after applying the proposed image-processing method to the original noisy simulated images. Results of

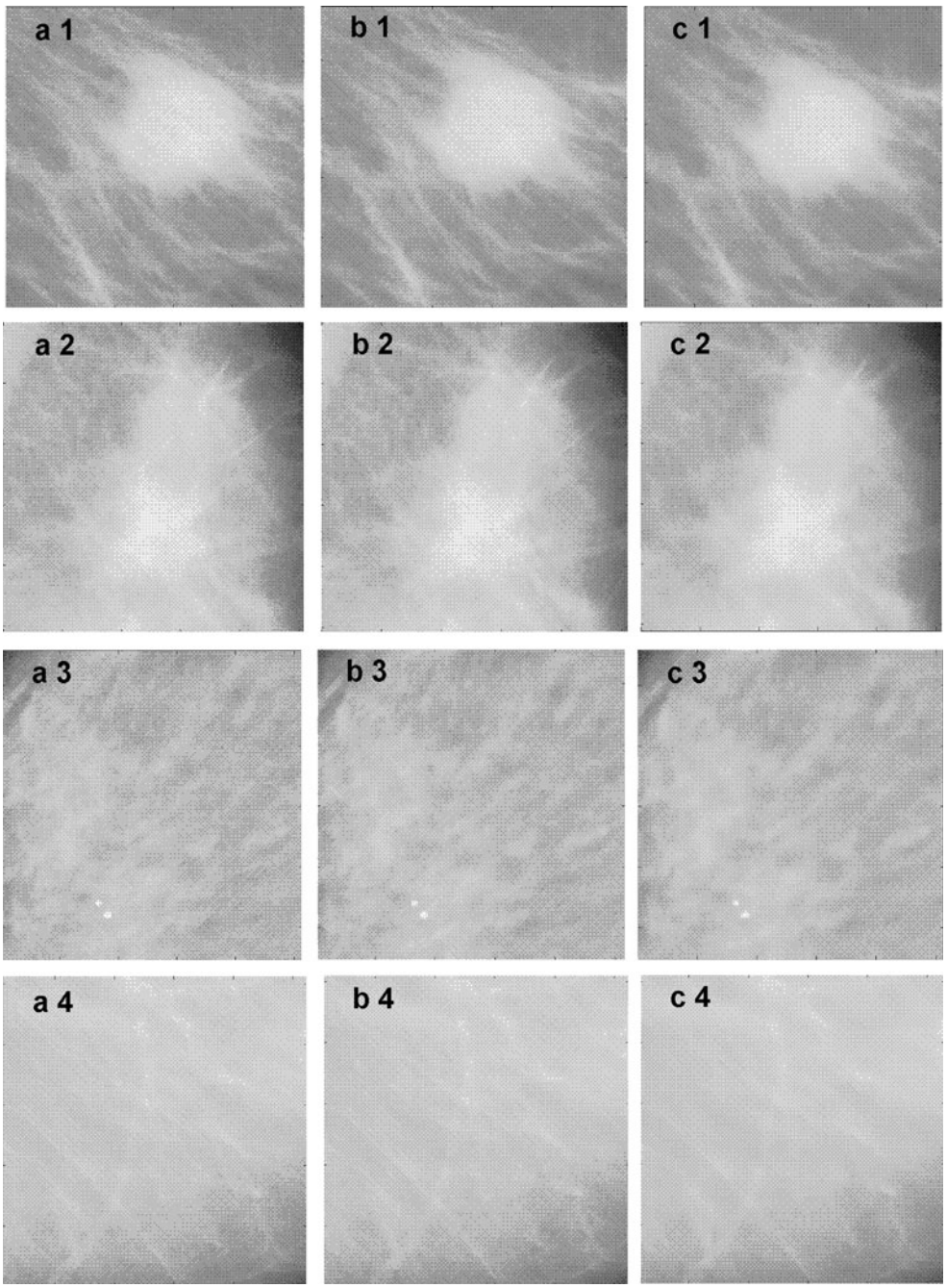

Fig. 5 Four examples of processing results for image denoising. **a** Original mammograms, **b** images processed with proposed UDWT method, and **c** images processed with conventional UDWT method. Shown at the *first* and *second rows* are two abnormal cases and shown at the *third* and *fourth rows* are two normal cases

quantitative assessment using the three measurement parameters are shown in Table 2. It is obvious from the three quality metrics shown in the table that the use of the proposed method significantly improved image quality in terms of noise.

Clinical Applications

Figure 5 illustrates four examples (enlarged parts) of processing results for image denoising. Shown on the left, middle, and right columns are original images, images processed with the proposed UDWT method, and images processed with the conventional UDWT method, respectively. Shown at the first and second rows are two abnormal cases and shown at the third and fourth rows are two normal cases.

An example of the results of applying the proposed method is shown in Fig. 6. Figure 6a, b is the original and the processed images, respectively. Perceptually, the processed image is less noisy. Figure 6c is the vertical wavelet coefficient of the subband at level 1, and Fig. 6d is the profile of the coefficient distribution traced from the line indicated on the image (Fig. 6c). Figure 6e shows the new coefficients of the subband at level 1 after performing the second iteration of the processing of the proposed method and Fig. 6f illustrates the profile of the coefficient distribution traced from the line indicated on the image (Fig. 6e). In comparison of the coefficient distributions shown in Fig. 6d, f, it is found that the noise has been significantly reduced. This demonstrates the effectiveness of our proposed method.

Visual Evaluation

The results of scoring for the three combinations by the seven observers are listed in Table 3. As described earlier, if the left image of the paired images (two-image combination) is poorer than the right image, the score obtained is a negative. From the preference scores shown on the rightmost column of Table 3, the images processed by the proposed UDWT method had the best quality. Figure 7

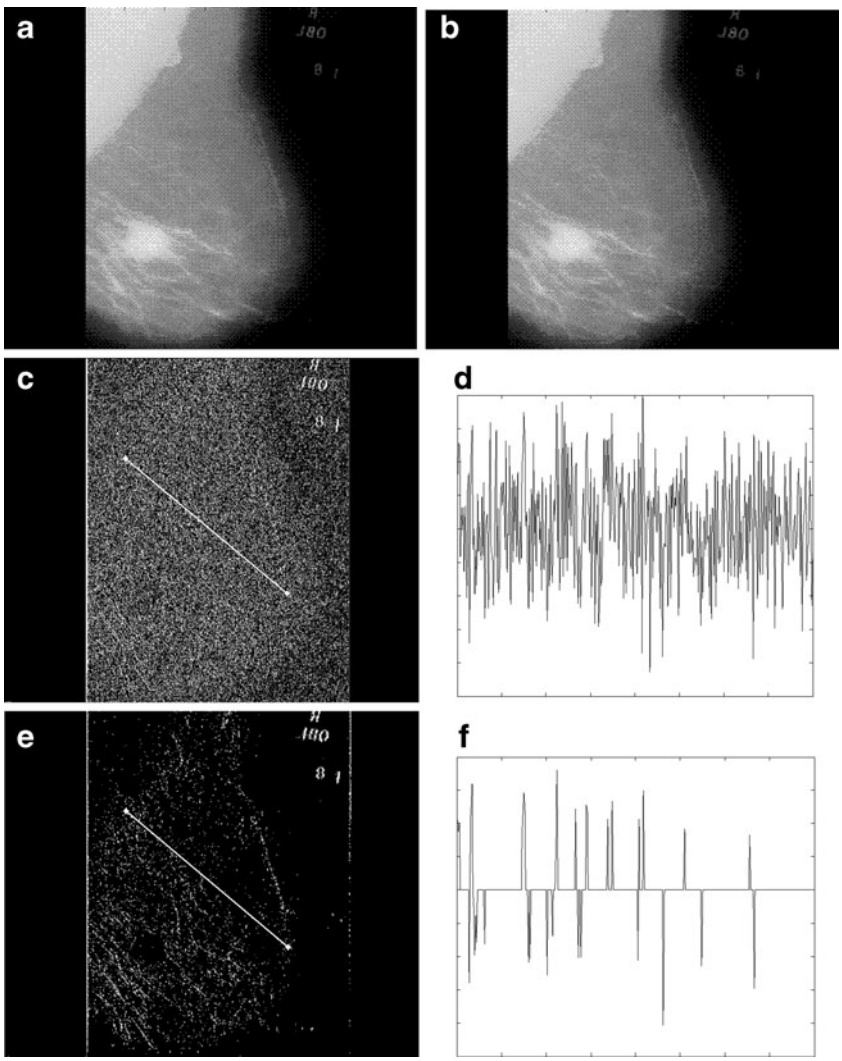

Fig. 6 An example showing images and plots of the detailed (*vertical*) coefficients. **a** Original image, **b** proposed-UDWT processed image, **c** vertical wavelet coefficient of the subband at level 1, **d** profile of the coefficient distribution traced from the *line* indicated in **c**, **e** new coefficients of the subbands at level 1, and **f** profile of the coefficient distribution traced from the *line* indicated in **e**

Table 3 Results of scoring for the three combinations by the seven observers

Combination	Observer							
	A	B	C	D	E	F	G	Sum
Original /C- UDWT	−1.2	−1.5	−1.0	−1.0	−1.2	−1.0	−1.0	−7.0
Original / P-UDWT	−2.0	−1.0	1.0	−0.2	−1.0	−1.0	−0.2	−4.4
C-UDWT /P- UDWT	−2.0	−2.0	−1.0	−1.8	−2.0	−1.0	−1.5	−12.0

C-UDWT: conventional undecimated discrete wavelet transform
P-UDWT: proposed undecimated discrete wavelet transform

illustrates visual evaluation results using Scheffe's method of paired comparisons. The results are depicted by a preference ranking map for the three image groups, i.e., original, conventional UDWT-processed, and proposed UDWT-processed image groups. The figures shown on the horizontal line of the map are average preference degrees of the three groups. The average preference degrees were obtained from the average main effects by use of the data shown in Table 3. The images processed by the proposed UDWT-method shows the highest ranking, followed by the conventional UDWT-method processed and the original images. A two-tailed F test was used to measure statistical significance. The differences between the proposed UDWT-method processed images and the conventional UDWT-method processed images were statistically significant ($P<0.01$). The differences between the conventional UDWT-method processed images and the original images were statistically significant ($P<0.05$), but there was no significant results with $P<0.01$.

Discussion

In the current study, we aimed to present a denoising method based on the UDWT for mammograms. By using our proposed UDWT technique, the computation time can be reduced to 2 s (personal computer, DELL, OPTIPLEX 960), approximately 1/10 of the computing time compared to the conventional UDWT method. The reason for enabling reduction of processing time lies in the following fact: in the conventional UDWT method, the decomposition and composition processes are usually conducted up to resolution level 4. That is, the method needs to process a total of 12 images (3 detailed coefficients for each of the 4-resolution levels) for wavelet transforms and inverse transforms and it results in time consuming. In contrast, the proposed UDWT method only needs to perform the process up to resolution level 2 and repeat the calculation one time. Therefore, only 6 images (3 detailed coefficients for each of the 2-resolution levels) were required for processing. As a result, the computing time using the proposed can be much reduced.

The proposed method computed the hierarchical correlation of the coefficient between the consecutive levels. The correlation value will become greater, if the coefficients are signal components. On the contrary, the correlation value becomes smaller, if the coefficients are noise components. Thus the discrimination between signal and noise becomes easier and more accurately as compared to the conventional UDWT method. As a result, an image with better quality could be obtained by use of the proposed method as compared to the conventional method.

We also conducted a visual evaluation experiment for the computer simulated images. The preference ranking was in the order of the proposed UDWT, conventional UDWT, and original simulated noisy image. The differences among the three images were statistically significant ($P<0.01$). The results of preference ranking were consistent with the clinical applications for mammograms.

In this study, we used MI as a physical measure of image quality. We also compared evaluation results in terms of MI against those in terms of MSE and SNR conventionally used for noise characterization. The results of the three measures were well consistent. It demonstrated the potential usefulness of the MI metric for image quality assessment.

This work has several limitations. First, in the simulation study, we used simulated noisy images presenting structural fibers on mammograms. However, typical breast pathologies are fibers (or fibrils), microcalcifications (or specks), and nodules (or masses). Therefore, further simulation studies that contain specks and masses on a phantom image are necessary. Second, the values shown in Eqs. 2 and 3 used in the procedure for determination of threshold value were empirically selected. A method for automated determination is desirable. Finally, we only took six wavelet basis

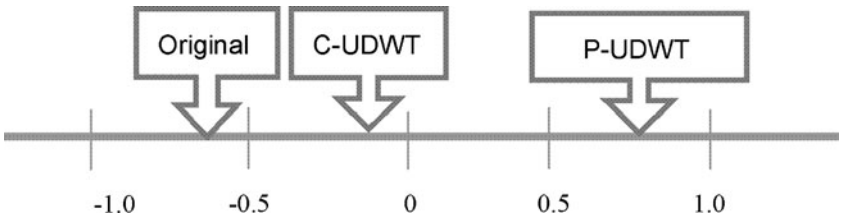

Fig. 7 Preference ranking map for the three image groups: original, conventional UDWT-processed, proposed UDWT-processed mammograms

functions into comparison. It may be possible to find a more suitable basis function than db2 basis function for the proposed UDWT method, if more basis functions are included for comparison. It was also noted that choice of wavelet basis function depends on the applications we use. Thus, the db2 basis function giving the best result is only limited to the present study.

Future work will focus on the combination of the proposed method with contrast enhancement method for further improvement in image quality of mammograms.

Conclusion

In this study, we presented an effective denoising method for reduction of the noise in mammographic images. The strength of the method was that we used hierarchical correlation of the coefficients of UDWT, together with iterative use of UDWT at adjacent levels 1 and 2. The advantage of the proposed method was that the algorithm is simple, fast, and gives better visual quality results. We examined the performance of the proposed method by comparing it with the conventional UDWT method in terms of processing time-consuming and image quality. Our results showed that the computation time can be reduced to less than 2 s (speed-up of factor 10) by using our proposed method. The results of visual assessment indicated that the images processed with the proposed UDWT method showed statistically significant superior image quality over those processed with the conventional UDWT method. Our research results demonstrated the superiority and effectiveness of the proposed approach. We used mutual information as an evaluation measure for selection of wavelet basis function. The assessment results were consistent with those measured with MSE and SNR. The results demonstrated the potential usefulness of mutual information served as an image quality metric.

Acknowledgments This research was supported in part by a Grant-in-Aid for Scientific Research (23602004) from the Japan Society for the Promotion of Sciences (JSPS). The authors also would like to thank the observers for their participation in visual evaluation.

References

1. Landis SH, Murray T, Bolden S, et al: Cancer statistics. CA Cancer J Clin 48(1): 6–29, 1998
2. American Cancer Society: Breast Cancer Facts & Figures 2009–2010. American Cancer Society. Atlanta, American Cancer Society, Inc: 1–36, 2009
3. Adel M, Zuwala D, Rasigni M, et al: Filtering noise on mammographic phantom images using local contrast modification functions. Image Vision Comput 26(9): 1219-1229, 2008
4. Sadaf A, Crystal P, Scaranelo A, et al: Performance of computer-aided detection applied to full-field digital mammography in detection of breast cancers. Eur J Radiol 77(3): 457-461, 2011
5. Tabar L, Yen MF, Vitak B, et al: Mammography service screening and mortality in breast cancer patients: 20 years follow-up before and after introduction of screening. Lancet 361(9367): 1405-1410, 2003
6. Dromain C, Thibault F, Muller S, et al: Dual-energy contrast-enhanced digital mammography: initial clinical results. Eur Radiol 21(3): 565-574, 2011
7. Wei J, Chan HP, Zhou C, et al: Computer-aided detection of breast masses: Four-view strategy for screen mammography. Med Phys 38(4): 1867-1876, 2011
8. Morton MJ, Whaley DH, Brandt KR, et al: Screening mammograms: Interpretation with computer-aided detection- prospective evaluation. Radiology 239(5): 375-383, 2006
9. Fenton JJ, Taplin SH, Carney PA, et al: Influence of computer-aided detection of performance of screen mammography. N Engl J Med 356(14): 1399-1409, 2007
10. Wang X, Li L, Xu W, et al: Improving performance of computer-aided detection of masses by incorporating bilateral mammographic density asymmetry: an assessment. Acad Radiol 19(3): 303-310, 2012
11. Samulski M, Hupse R, Boetes C, et al: Using computer-aided detection in mammography as a decision support. Eur Radiol 20 (10): 2323-2330, 2010
12. Tourassi GD, Ike III R, Singh S, et al: Evaluating the effect of image preprocessing on an information-theoretic CAD system in mammography. Acad Radiol 15(5): 626-634, 2008
13. Mencattini A, Salmeri M, Rabottino G, et al: Metrological characterization of a CADx system for the classification of breast masses in mammograms. IEEE Trans on Instr and Meas 59: 2792-2799, 2010
14. Mencattini A, Salmeri M: Metrological assessment of a CAD system for the early diagnosis of breast cancer in digital mammography. In: Mammography –Recent Advances. InTech, Mar. 2012, pp. 293–320
15. Baydush AH, Catarious DM, Lo JY, et al: Incorporation of a Laguerre-Gauss channelized hotelling observer for false-positive reduction in a mammographic mass CAD system. J Digit Imaging 20:196-202, 2007
16. Camilus KS, Govindan VK, Sathidevi PS: Computer-aided identification of the pectoral muscle in digitized mammograms. J Digit Imaging 23: 562-580, 2010
17. Matheus BRN, Schiabel H: Online mammographic images database for development and comparison of CAD schemes. J Digit Imaging 24: 500-506, 2011
18. Bozek J, Mustra M, Delac K, et al: A survey of image processing algorithms in digital mammography. Studies in computational intelligence 231: 631-657, 2009
19. Zanca F, Jacobs J, Ongeval CV, et al: Evaluation of clinical image processing algorithms used in digital mammography. Med Phys 36 (3): 765-775, 2009
20. Scharcanski J, Jung CR: Denoising and enhancing digital mammographic images for visual screening. Comput Med Imaging Graphics 30(4): 243-254, 2006
21. Zhang X, Xie H: Mammograms enhancement and denoising using generalized Gaussian mixture model in nonsubsampled contourlet transform domain. Journal of Multimedia 4(6): 389-396, 2009
22. Jung CR, Scharcanski T: Wavelet transform approach to adaptive image denoising and enhancement. J Electron Imaging 13(2): 278–285, 2004
23. Kappadath SC, Shaw CC: Dual-energy digital mammography for calcification imaging: noise reduction techniques. Phys Med Biol 53(19): 5421–5443, 2008
24. Bouwman R, Young K, Lazzari B, et al: An alternative method for noise analysis using pixel variance as part of quality control

procedures on digital mammography systems. Phys Med Biol 54 (22): 6809–6822, 2009
25. Mayo P, Rodenas F, Verdu G: Comparing methods to denoise mammographic images. Proc of the 26th Annual Intl Conference of the Engineering on medicine and Biology Society. 1: 247–250, 2004
26. McLoughlin KJ, Bones PJ, Karssemeijer N: Noise equalization for detection of microcalcification clusters in direct digital mammogram images. IEEE Trans Med Imaging 23(3):313-320, 2004
27. Starck JL, Candes EJ, Donoho DL: The curvelet transform for image denoising. IEEE Trans Image Process 11(6): 670-684, 2002
28. Adel M, Zuwala D, Rasigni M, et al: Noise reduction on mammographic phantom images. Electronic Letters on Computer Vision and Image Analysis 5(4): 64-74, 2006
29. Mencattini M, Salmeri M, Lojacono R, et al: Mammographic images enhancement and denoising for breast cancer detection using dyadic wavelet processing. IEEE Trans Instrum Meas 57 (7): 1422-1430, 2008
30. Xu Y, Weaver JB, Healy DM, et al: Wavelet transform domain filters: A spatially selective noise filtration technique. IEEE Trans. Image Process 3(6): 747-758, 1994
31. Fodor IK, Kamath C: Denoising through wavelet shrinkage: an empirical study, J Electron Imaging 12 (1): 151-160, 2003
32. Sampat MP, Whitman GJ, Bovic AC, et al: Comparison of algorithms to enhance spicules of speculated masses on mammography. J Digit Imaging 21: 9-17, 2008
33. Romualdo LCS, Vieira MAC, Schiabel H, et al: Mammographic imaging denoising and enhancement using the anscombe transformation, adaptive wiener filtering, and the modulation transfer function. J Digit Imaging (on line first) (doi:10.1007/s10278-012-9507-1)
34. Ferreira CBR, Borges DL: Analysis of mammogram classification using a wavelet transform decomposition. Pattern Recognition Letters 24(7): 973-982, 2003
35. Cho D, Bui TD, Chen G: Image denoising based on wavelet shrinkage using neighbor and level dependency. Int J Wavelets Multiresolut Inf Process 7: 299-311, 2009
36. Gyaourove A, Kamath C, Fodor IK: Undecimated wavelet transforms for image de-noising. Report Lawrence Livermore National Laboratory 12: 1-12, 2002.
37. Fowler JE: The redundant discrete wavelet transform and additive noise. IEEE Signal Processing Letters 12(9): 629-632, 2005
38. Starck JL, Fadili J, Murtagh F: The undecimated wavelet decomposition and its reconstruction. IEEE Trans Image Process 16(2): 297-309, 2007
39. Wang XY, Yang HY, Fu ZK: A new wavelet-based image denoising using undecimated discrete wavelet transform and least square support vector machine. Expert Systems with Applications 37(10): 7040-7049, 2010
40. Mencattini A, Salmeri M, Caselli F, et al: Subband variance computation of homoscedastic additive noise in discrete dyadic wavelet transform. Int J Wavelets Multiresolut Inf Process 6: 895-906, 2008
41. Mencattini A, Rabottino G, Salmeri M, et al: Denoising and enhancement of mammographic images under the assumption of heteroscedastic additive noise by an optimal subband thresholding. Int J Wavelets Multiresolut Inf Process 8: 713-741, 2010
42. Zhao P, Shang Z, Zhao C: Image denoising based on Gaussian and non-gaussian assumption. Int J Wavelets Multiresolut Inf Process 10: 1250014 (11 pages), 2012
43. Huang Z, Fang B, He X, et al: Image denoising based on the dyadic wavelet transform and improved threshold. Int J Wavelets Multiresolut Inf Process 7: 269-380, 2009
44. Liu TT, Fraser-Smith AC: Detection of transient in 1/f noise with the undecimated discrete wavelet transform. IEEE Trans Signal Processing 48(5): 1458-1462, 2000
45. Addison PS: The illustrated wavelet transform handbook. London: IOP, 2002
46. Donoho D, Johnstone I: Ideal spatial adaptation by wavelet shrinkage. Biometrika 81(3): 425-455, 1994
47. Coifman RR, Donoho DL: Translation invariant de-noising. Lecture Notes in Statistics 103: 125-150, 1995
48. Matsuyama E, Tsai DY, Lee Y: Mutual information-based evaluation of image quality with its preliminary application to assessment of medical imaging systems. J Electron Imaging 18(3): 033011, 1-11, 2009
49. Matsuyama E, Tsai DY, Lee Y, et al: Using mutual information to evaluate performance of medical imaging systems. Health 2(4): 279-285, 2010
50. Singh BN, Tiwari AK: Optimal selection of wavelet basis function applied to ECG signal denoising. Digit Signal Process 16(3): 257-287, 2006
51. Tsai DY, Lee Y, Matsuyama E: Information entropy measure for evaluation of image quality. J Digit Imaging 21(3):338-347, 2008
52. Japanese Society of Medical Imaging Technology. Available at: http://www.jamit.jp/cad-committe/caddbinfo. Accessed 11January 2012
53. Scheffe H: The Analysis of variance. New York: John Wiley & Sons, 1959
54. Canavos GC, Koutrouvelis JA: An Introduction to the design & analysis of experiments. Pearson Prentice Hall, 2008 (eBook)